SIA

Nanoalignment mask fabricated directly on Si by AFM[†]

WenHao Huang,[1*] Xueming Dang,[1] Qiao Hu,[1] Yi Xia,[1] Marta Telllo,[2] Montserrat Calleja,[2] Ricardo García,[2] J. M. Gómez-Rodńguez[3] and A. Baro[3]

[1] Open Laboratory of Bond Selective Chemistry, Department of Precision Machinery and Instrumentation, University of Science and Technology of China, 230026 HeFei, China

[2] Instituto de Microelectrónica de Madrid,CSIC,26760 Tres Cantos, Madrid, Spain

[3] Dept. Física Materia Condensada,C-III Universidad Autónoma de Madrid, 28049-Madrid, Spain

The alignment mask with submicrometre and nanometre sensitivity is very important and useful in the microelectronics industry and for nanoscience and technology in the near future. Here we report for the first time a nanoalignment mask that has been fabricated directly on Si by atomic force microscopy. Copyright © 2001 John Wiley & Sons, Ltd.

INTRODUCTION

The alignment mask with submicrometre and nanometre sensitivity is very important and useful in the microelectronics industry and for nanoscience and technology.[1–5] It is well known that micropositioning and alignment also are used widely in the field of micro electronic mechanical system (MEMS) and precision engineering. With the development of technologies, it is required that masks be designed and fabricated with higher precision. In this article we report for the first time a nanoalignment mask that has been fabricated directly on Si by atomic force microscopy (AFM). The design concept, manufacturing process and characterization are described.

DESIGN CONSIDERATION

A special coded two-dimensional grid is designed. It is expected theoretically that when the two grids are in the correct alignment position the maximum output can be obtained. If there is a small relative disalignment the output will fall rapidly. The principle is described in detail in Ref. 6. Figure 1 shows the two-dimensional grid code and the output change with the relative displacement. The amplitude of the central peak is several times bigger than any other subpeaks and the width of the peak is only one unit of the grid. Within the peak, the intensity changes linearly. This central sharp peak can be used as a precision mark in a lithographic system with very high sensitivity and accuracy.

FABRICATION PROCESS

We use a local oxidation method by AFM to write the pattern on a silicon surface.[7] Fabrication was performed with a conducting AFM tip operated in non-contact mode
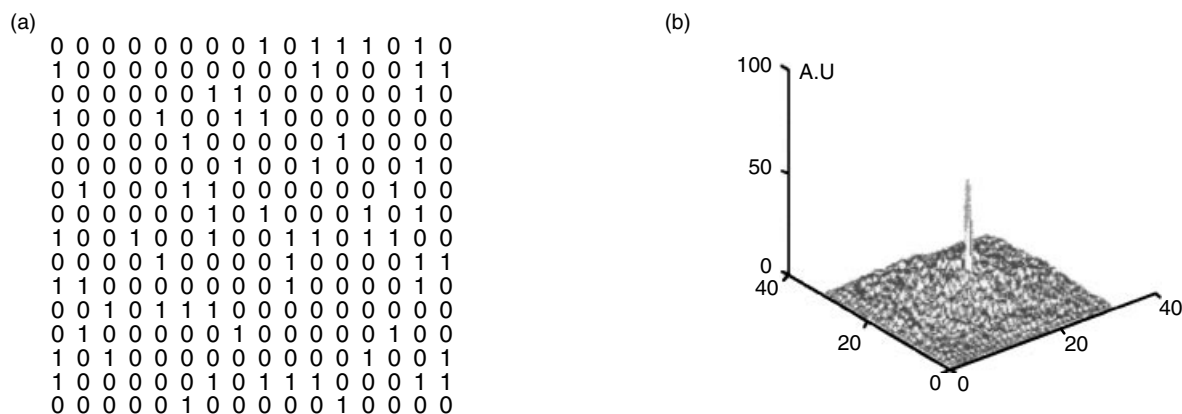
(a)
```
0 0 0 0 0 0 0 0 1 0 1 1 1 0 1 0
1 0 0 0 0 0 0 0 0 1 0 0 0 1 1
0 0 0 0 0 0 1 1 0 0 0 0 0 1 0
1 0 0 0 1 0 0 1 1 0 0 0 0 0 0
0 0 0 0 0 1 0 0 0 0 1 0 0 0 0
0 0 0 0 0 0 1 0 0 1 0 0 0 1 0
0 1 0 0 0 1 1 0 0 0 0 0 1 0 0
0 0 0 0 0 1 0 1 0 0 0 1 0 1 0
1 0 0 1 0 0 1 0 0 1 1 0 1 1 0 0
0 0 0 0 1 0 0 0 0 1 0 0 0 0 1 1
1 1 0 0 0 0 0 0 1 0 0 0 0 1 0
0 0 1 0 1 1 1 0 0 0 0 0 0 0 0
0 1 0 0 0 0 1 0 0 0 0 0 1 0 0
1 0 1 0 0 0 0 0 0 0 0 1 0 0 1
1 0 0 0 0 1 0 1 1 1 0 0 0 1 1
0 0 0 0 0 1 0 0 0 0 1 0 0 0 0
```

(b)

Figure 1. (a) The code of the theoretic grid. (b) The calculated output change with the relative displacement. The units of the *x*- and *y*-axes are the numbers of the codes.
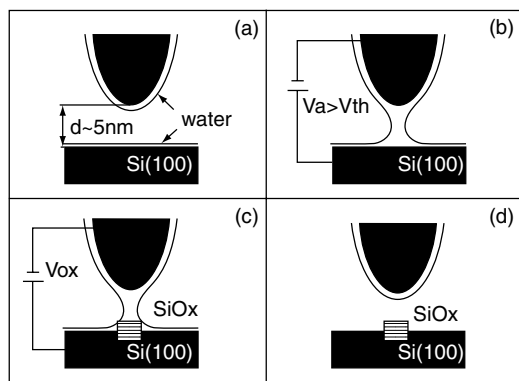
Figure 2. Steps in the oxidation of Si(100) with a dynamic force microscope. (a) An oscillating tip approaches the surface up to a minimum equilibrium distance of ~5 nm. (b) An external voltage V_a polarizes the water monolayers adsorbed onto the surface. If V_a is above the threshold voltage V_{th} a bridge is formed. (c) A voltage pulse V_{ox} is applied to induce oxidation of the silicon. (d) The tip is withdrawn and the dot is imaged.
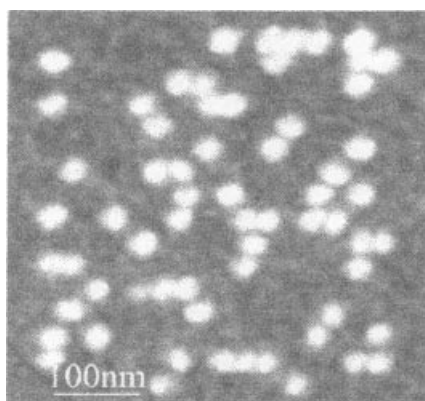

Figure 3. An AFM image of the fabricated grid according to the code in Fig. 1. The bright dots correspond to the '1' in Fig. 1. The dot size is ~30 nm × 30 nm and the height is <2 nm.

(Nanoscope III, Digital Instruments), with additional circuits to perform the oxidation.

The sample was p-type Si(100) with a resistivity of $14\ \Omega \cdot cm$. To eliminate organic contaminants, the sample was sonicated for 60 s first in acetone and then in ethanol. For environmental control, the microscope was placed into a closed box with an inlet for dry and H_2O-saturated nitrogen. Owing to exposure to air, the surface of silicon has a native oxide layer of ~2 nm.

Several steps (schematized in Fig. 2) are required to form liquid bridges on Si(100) surfaces. First, a few monolayers of water are absorbed onto the surface [Fig. 2(a)]. Next, a force microscope cantilever/tip is oscillated a few nanometres above the sample surface. Then, an external voltage pulse (V_a) of several milliseconds is applied. The electrical field (pulse) polarizes the water layer in the proximity of the tip's apex. The voltage is above a certain threshold value (V_{th}) that depends on the tip-to-sample separation. In our fabrication, the tip-to-sample separation is ~5 nm, (V_{th}) is 11 V and the applied voltage V_a is a 0.5 ms pulse of 18 V.[8] A water bridge between the tip and the sample is formed [Fig. 2(b)]. Once the water bridge is formed, another voltage pulse V_{ox} (sample positive) is applied to grow the oxide. The V_{ox} in our system is a 0.3 s pulse of 8 V. According to the two-dimensional coded grid (Fig. 1), the tip of the microscopy was driven and the pattern was oxidized on the surface of silicon. Then we obtained a coded grid of 16×16 elements and the size of each element is 30 nm×30 nm. An AFM image of this is shown in Fig. 3. The lateral size of each individual dot is ~30 nm and the height is <2 nm.

CHARACTERIZATION

Because the diffraction effect will be strong due to the reduced dimension, it is more difficult to use the real optical method[9] to measure the output and verify the principle, so we use autocorrelation of the real AFM image of the 16×16 oxidation grid. Figure 4 shows the autocorrelation result. It is clear that the output of the real grid is in good agreement with the theoretical output in Fig. 1. The width of the peak is ~30 nm within the peak and the output is linear.
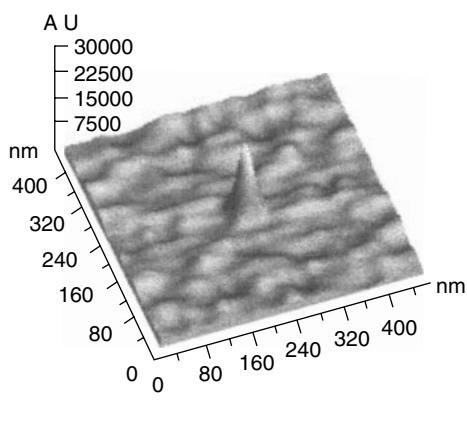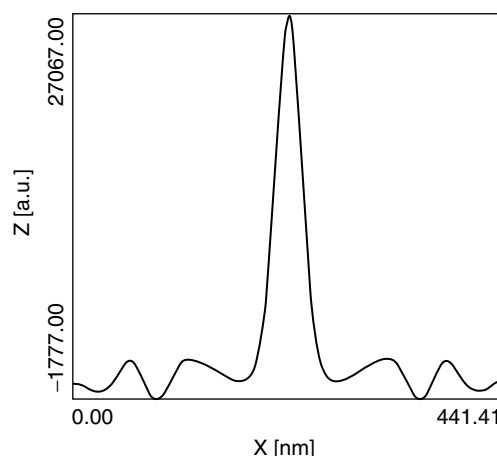

Figure 4. (a) Image of autocorrelation of the real AFM image of the 16×16 oxidation grid mask. (b) Profile of the middle section of the autocorrelation image.

SIA

Acknowledgements

REFERENCES

1. Potenza G. *Microelectron. Eng.* 1992; **17**: 59.
2. Horiuchi T, Saito Y, Komatsu K. *Microelectron. Eng.* 1996; **30**: 219.
3. Malek K, Jackson KH, Bonivert WD, Kruby J. *J. Micromech. Microeng.* 1996; **2**: 228.
4. Wenwei W, Qiao H, Xiaohua W, Wenhao H. *Proc. China–Japan Bilateral Symposium on Advanced Manufacturing Engineering*. Yellow Mountain City: P.R. China, 1998; 145–149.
5. Flanders DC, Smith HI. *Appl. Phys. Lett.* 1977; **31**: 426.
6. Qiao H, Wenwei W, Wenhao H, Zhi L. *J. Chin. Electron Microsc. Soci.* 1999; **18**(1): 137 (in Chinese).
7. Garcia R, Calleja M, Rohrer H. *J. Appl. Phys.* 1999; **86**: 1898.
8. Garcia R., Calleja M, Perez-Murano F. *Appl. Phys. Lett.* 1998; **72**: 2295.
9. Wenhao H, Huqiao X. *Proc. First EUSPEN Topic Conference on Fabrication and Metrology in Nanotechnology*, Denmark, 2000; 268–271.